JOURNAL OF MATERIALS SCIENCE **35** (2000) 455–463

Optical and electrical properties of conjugated oligo(arylenes)

W. CZERWIŃSKI*
Faculty of Chemistry, N. Copernicus University, Gagarina 7, 87-100 Toruń, Poland

L. Å. LINDÉN, J. F. RABEK
Polymer Research Group, Department of Dental Biomaterials Science, Karolinska Institute (Royal Academy of Medicine), Box 4046, 141 04 Huddinge (Stockholm), Sweden

New conductive soluble oligo(*p*-phenylene), oligo(thiophene), oligo(*p*-phenylene-thiophene) (4 : 1) (1 : 1) (1 : 4), oligo(*p*-phenylene-sulphide), oligo(*p*-phenylene-selenide), oligo(*p*-diphenylene-sulphide) and oligo(*p*-diphenylene selenide) were synthesized. Structural, optical and electrical characteristics of these oligomers have been determined. The optical and electrical properties are dependent on the oligomers' structures. The conductivities of these oligomers are low, between 10^{-4} and 10^{-12} S m^{-1}. However, there is an increase after doping them with iodine. These soluble oligomers can be used for production of active components in opto-electronic devices.

1. Introduction

Conjugated polymers have remarkable electronic properties [1–4]. They are intrinsically conducting, and are actively studied for their electron excitations and motions in 1-D structures. Conjugated polymers have been used as active materials in field-effect-transistors [5–9], light-emitting diodes [10–15], and in nonlinear optics [16–19]. Recent band structure calculations [20, 21] have shown that a fine tuning of energy gap can be done by construction of regular block copolymers as a combination of sequences of polymer A and B with different energy gap (E_g) values. An increase of the nonlinear optical responses (resonant χ^3-third-order op. nonlinearities) can be obtained when alternating low and high energy gap polymer sequences or fragments are introduced along the polymer chain [20]. Besides the difference at the energy gaps, the length and regularity of blocks are also important [21, 22]. However, production of exactly regular-sequenced copolymers is rather difficult and restricted in practice. It was recently shown that in the case of block copolymers, with alternating aromatic and quinoic heteroarylene moietes in the main chain, the intrinsinc bandgaps (E_g) were significantly smaller than those found for parent polymers [23]. Soluble conductive polymer materials may, beside wide applications in the electrical and electronic industries, also lead to new applications in dentistry in order to reduce and/or remove galvanic effects of metallic restorative materials [24].

Lately, the interest in conjugated oligomers is growing rapidly because of the good processability and semiconducting properties close to (and sometimes better than) those of parent polymers (e.g. regarding mobility of carriers) [7–10, 15].

The aim of this work was to obtain and investigate the physico-chemical properties of short-chain soluble conductive polymers with different energy gaps, and with such reactive end groups that will give a possibility to attatch them to alternating block copolymers.

2. Experimental

Different oligomers were prepared from: 1,4-dibromobenzene, 4,4-dibromobiphenylene, 2,5-dibromothiophene, sodium sulfide, sodium selenide (prepared with an "*in situ* method" from selenium powder) and magnesium-Grignard chips respectively. All reagents were from Aldrich.

Oligomers of: *p*-phenylene (oligo(*p*P)), thiophene (oligo(T)), *p*-phenylene-thiophene (oligo(*p*P-T)) (Table I) were obtained by coupling reactions between Grignard reagents of 1,4-dibromobenzene and/or 2,5-dibromothiophene, catalyzed by organo-nickel complexes in THF solution [3]. Different oligomers of *p*-phenylene-thiophene (Table I) were synthesized by taking different molar ratios (4 : 1, 1 : 1 and 1 : 4) of 1,4-dibromobenzene and 2,5-dibromothiophene in the reactions.

Oligomers of: *p*-phenylene-sulfide (oligo(*p*P-S)), *p*-phenylene-selenide (oligo(*p*P-Se)), *p*-diphenylene-sulphide (oligo(*p*DP-S)) and *p*-diphenylene-selenide (oligo(*p*DP-Se)) (Table I) were synthesized by reaction of 1,4-dibromobenzene and 4,4-dibromobiphenylene with sodium sulfide and sodium selenide, respectively, in DMF solutions [25, 26]. Crude products were precipitated with methanol, purified from NaBr and dissolved in tetrahydrofuran, again to collect soluble fraction of the products.

* To whom all correspondence should be directed.

TABLE I Number ($\overline{M}_n$) and weight ($\overline{M}_w$) average molecular weights, average polydispersity index (PD), and average number of repeating units (n) for different oligomers

Sample	$\overline{M}_n$	$\overline{M}_w$	PD	n
oligo(T)	856	1370	1.60	8–9
oligo(*p*P)	730	1248	1.71	7–8
oligo(*p*P:T) = 4 : 1	1193	2326	1.95	12–13
oligo(*p*P:T) = 1 : 1	953	1811	1.90	10
oligo(*p*P:T) = 1 : 4	1177	2219	1.90	11–12
oligo(*p*P-S)	737	980	1.33	7
oligo(*p*P-Se)	812	1076	1.32	5–6
oligo(*p*DP-S)	856	1057	1.24	4–5
oligo(*p*DP-Se)	792	1006	1.27	3

oligo(*p*-phenylene) oligo(*p*P)

oligo(thiophene) oligo(T)

oligo(*p*-phenylene-thiophene) oligo(*p*P-T)

oligo(*p*-phenylene-sulphide) oligo(*p*P-S)

oligo(*p*-phenylene-selenide) oligo(*p*P-Se)

oligo(*p*-diphenylene-sulphide) oligo(*p*DP-S)

oligo(*p*-diphenylene-selenide) oligo(*p*DP-Se)

Molecular weights and polydispersity indexes (PD) of synthesized oligomers were determined in THF using a GPC, Model GP 8810, (Spectra Physics) equipped with a SP-column calibrated with polystyrene standards. Oligomers with PD > 2 were additionally fractionated by precipitation in methanol.

UV-vis and IR absorption spectra were recorded with Beckman 7500 UV-vis and FTIR Perkin Elmer 1650 spectrometers, respectively. Fluorescence emission spectra were measured with a Jasco FP-4 fluorescence spectrometer. High resolution ^{13}C NMR spectra in solid state were recorded with a laboratory made spectrometer using cross polarization (CP)/magic angle spining (MAS) and depolar-dephasing (DD) experimental techniques, described in detail elsewhere [27]. Mass spectra were recorded with a Varian MAT 711 spectrometer with accelerating voltage 6 + 3 kV. Electron diffraction spectra were measured with a 170-keV laboratory made spectrometer [28].

Current-voltage characteristics and conductivity measurements were measured using a two-point probe and a solid state electrometer (Type 610 C Keithley Instrument) on pressed tablets (at 3.92×10^6 Pa) with vacuum Au metalized junctions. Measurements were carried out in the dark at different temperatures. The doping process (in which most polyiodide ions are in the form of the I_{3^-}) was carried out with iodine vapour at (1333 Pa) according to the literature [29].

3. Results and discussion

3.1. Structure of oligomers

All synthesized oligomers are characterized by low molecular weights and broad molecular weight distributions (MWD) (PD > 1) (Table I). In Fig. 1 an example of the MWD for oligo(*p*P) is shown. Oligo(*p*P-T)s

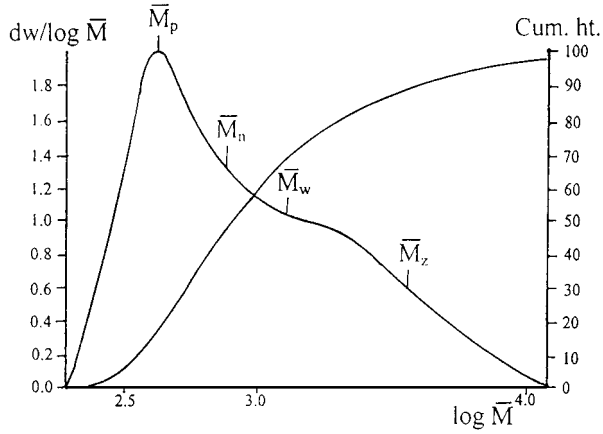

Figure 1 GPC chromatogram of poly(*p*P) in THF solution.

with different ratios of *p*-phenylene : thiophene show the same PD = 1.90 and the highest M_n and M_w. These oligomers were synthesized in order to tune the energy gap between differently distributed *p*-phenylene and thiophene blocks.

IR spectra of oligo(*p*P) and oligo(T) are shown in Fig. 2. Strong absorptions at 808 cm^{-1} (oligo(*p*P)) and 791 cm^{-1} (oligo(T)) can be attributed to the C–H out-of-plane vibration in phenylene rings (1–4 coupled) [30, 31], and in the thienylene rings (Cβ-H, α-α coupling) [32, 33], respectively.

In the case of oligo(T) (Fig. 2), in the range of 4000–1600 cm^{-1} (not shown here), two bands at 3100 (mild) and 3064 cm^{-1} (strong) are assigned to the Cβ-H stretching vibration. Bands at 3050 and 1076 cm^{-1} attributed to the Cα-H [33] are absent in the IR spectrum, because the oligo-T is terminated mainly by Br atoms, and the Cα-Br band appears at 968 cm^{-1} instead. The positions of two bands, at 1220 cm^{-1} (C–C vibration) and 1047 cm^{-1} (Cβ-H bending vibration), are the same as reported elsewhere [33]. The presence of two other bands at 832 and 689 cm^{-1} are assigned to monosubstituted thiophene rings [33], and indicate that not all terminal rings are ended by bromine atoms, however their concentration must be low.

In the case of oligo(P) (Fig. 2), all bands are the same as reported earlier for oligo(P) and poly(*p*-phenylene), also synthesized from 1,4-dibromobenzene [3, 30]. The presence of the strong band at 1070 cm^{-1} (C–Br vibration) suggests that that dominant terminal phenylene rings are ended with bromine atoms [3].

IR spectrum of for example oligo(*p*P-T) (1 : 1) is shown in Fig. 3. The spectrum exhibits several bands characteristic of vibrational modes of phenylene and thienylene units respectively. Two peaks with the same intensity, at 810 and 797 cm^{-1}, can be attributed to the C–H out-of-plane vibrations in phenylene rings (1–4 coupled) and thienylene rings (Cβ-H, α-α coupling), respectively. The strong 1071 cm^{-1} band can be attributed to the Cα-Br vibrations in the terminal groups in oligo-*p*P. The band originating from Cα-Br in oligo-T is seen as a shoulder on a new band near 956 cm^{-1}. This leads to the assumption that the oligo(*p*P-T)s are ended by bromophenylene rather than by bromothienylene groups.

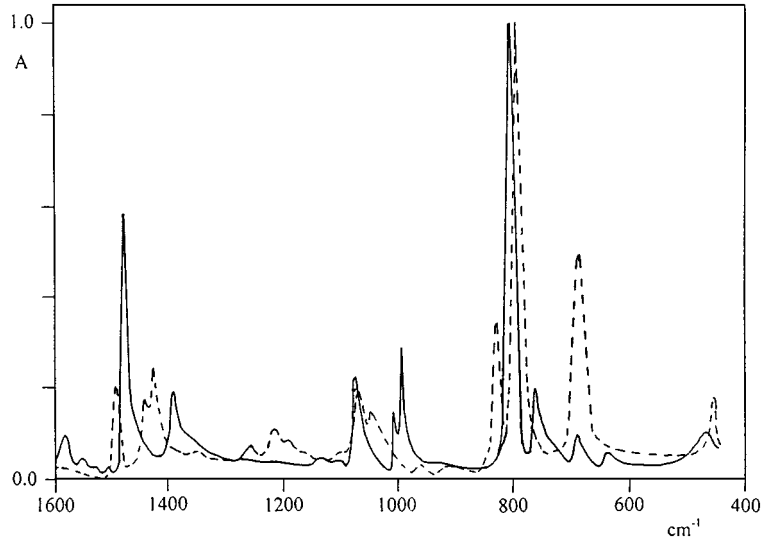

Figure 2 FTIR absorption spectra of: (—) oligo(*p*P) and (- -) oligo(T).

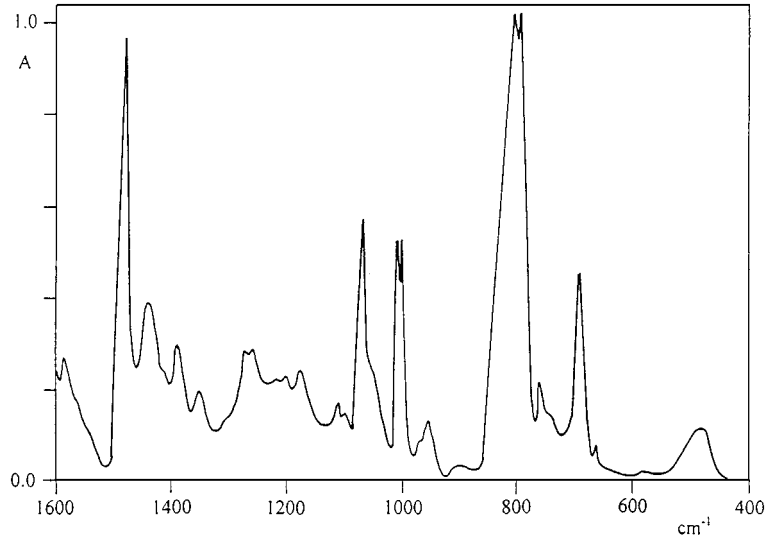

Figure 3 FTIR absorption spectrum of oligo(*p*P-T) (1 : 1).

The ^{13}C-NMR spectra of the oligo(*p*P), oligo(T) and oligo(*p*P-T) (1 : 1) in solid state (CP/MAS technique) are shown in Fig. 4. The spectrum of oligo(*p*P) has two resonance lines with different intensities (Fig. 4a). The low-field resonance line (137 ppm) in the oligo(*p*P) spectrum is characteristic for non-protonic carbons in positions 1 and 4, which links phenylene rings together. The 127 ppm resonance line is attributed to protonic carbons 2,3,5,6, and has a higher intensity because the concentration of protonic carbons in the oligophenylene structure is two times higher than that of non-protonic carbons. The spectrum of oligo(T) also shows two very intense, well resolved lines (Fig. 4b). The use of depolar dephasing (DD) techniques allowed us to ascribe these lines to the carbons linked to thienylene units (137.5 ppm) and unbonded atoms (3 and 4 carbons) located at 126.5 ppm. The presence of only two peaks in the oligo(T) spectrum shows that the β-branching (loss of Π-conjugation) for oligomers with a number (n) of thiophene units higher than 6, for chemical oxidative [8] and/or electrochemical [34] polymerizations of thiophene reported in the literature, does not exist. In the case of oligo-T($n = 7$–8) presented in our paper, only α-coupling has been observed.

The ^{13}C NMR-spectrum of oligo(*p*P-T) (1 : 1) is shown in Fig. 4c. This spectrum shows four resonance lines with different intensities. Two lines 127 and 137 ppm are attributed to carbons 3,4,7,8,10,11 present in the parent structures of oligo-P and oligo-T. Two other lines 143 and 134 ppm are characteristic for carbons linked in phenylene (carbon 6) with thienylene (carbon 5) rings. The presence of further lines showed that oligo(*p*P-T) has a random structure. The presence of lines from 2 and 9 carbons, and 5 and 6 carbons respectively exclude alternating and block structures in the oligo(*p*P-T). Other oligo(*p*P-T)s, (4 : 1 and 1 : 4) exhibit similar, 4 lines spectra with different peak intensities that are characteristic for the composition and the random structures in these oligomers.

The IR spectrum of oligo(*p*P-Se) (not shown here) showed two strong absorption bands at 1067 and 498 cm^{-1} which are assigned to Cα-Br terminal groups in oligo(*p*P-Se) and Cα-Se stretching vibration, respectively.

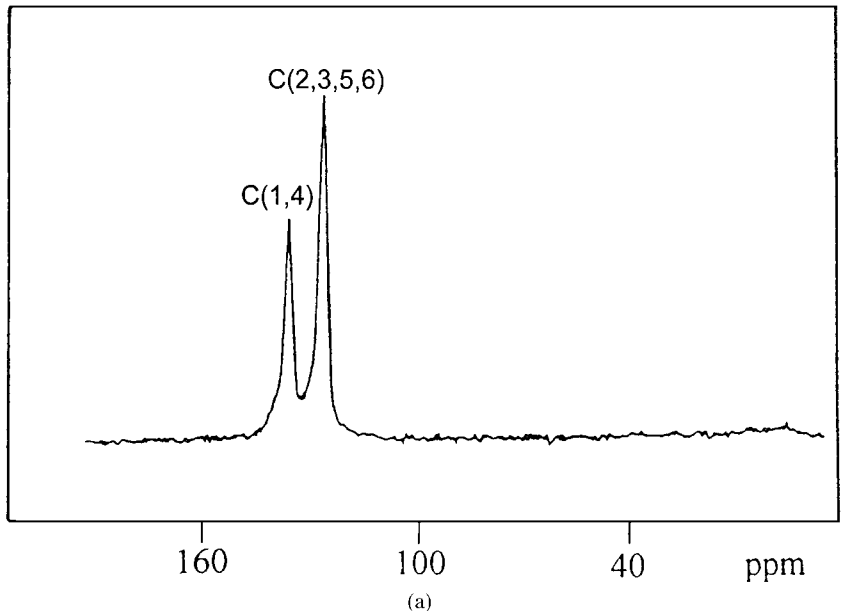

(a)

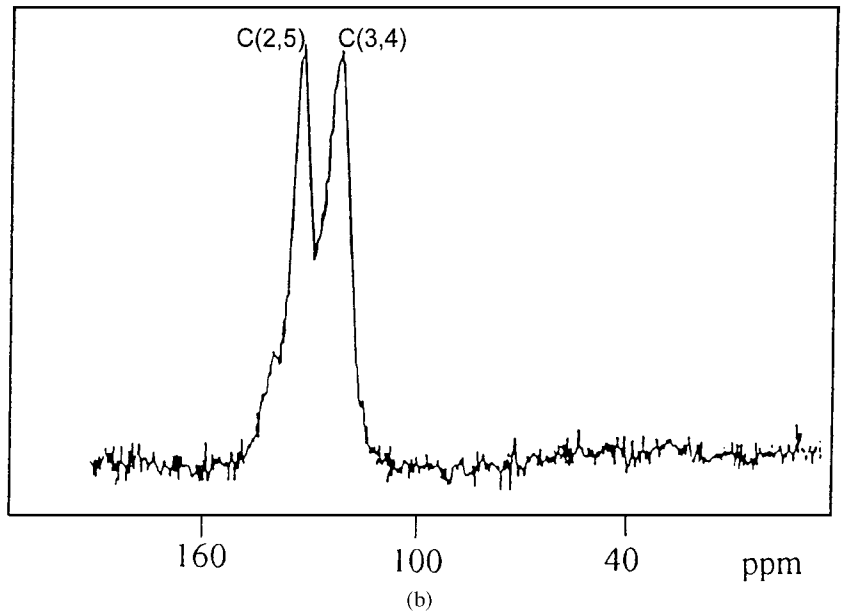

(b)

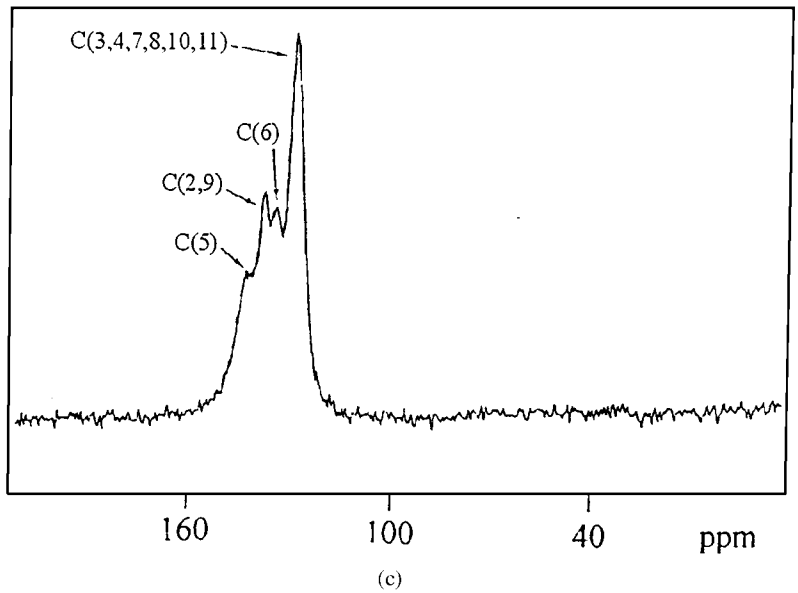

(c)

Figure 4 ^{13}C NMR spectra of: (a) oligo(*p*P); (b) oligo(T) and (c) oligo(*p*P-T) (1 : 1).

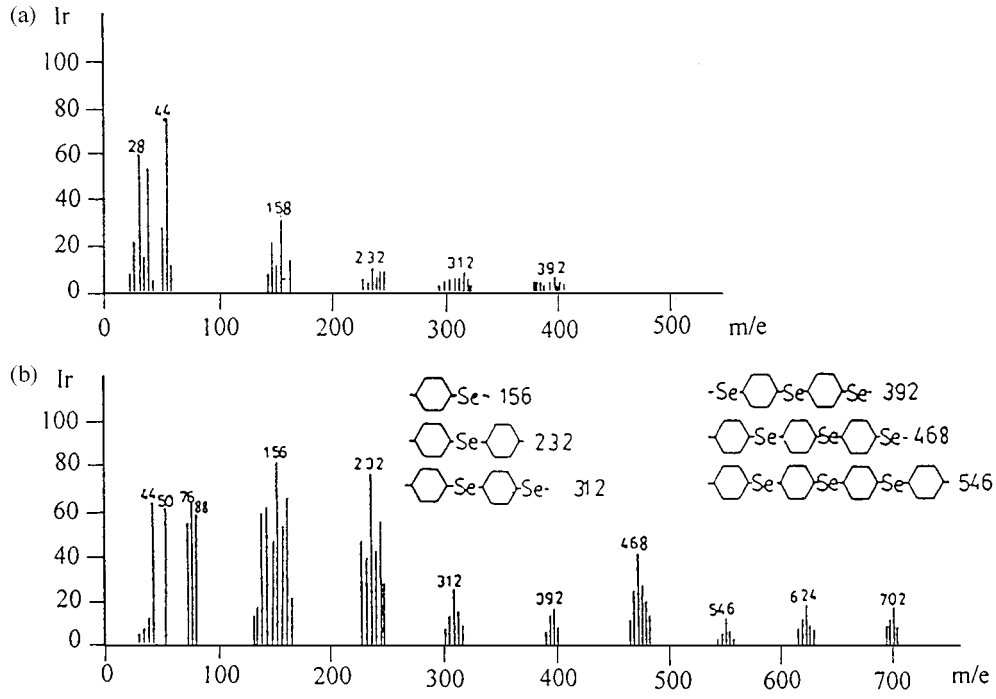

Figure 5 Mass spectra of oligo(*p*P-Se): (a) $n = 6$ and (b) $n = 23$.

The far-IR spectrum of oligo(*p*P-Se) shows absence of the band Se-Se at 290 cm^{-1} which may indicate a change in the conjugation between π-electrons of the adjacent phenylene rings [25]. The mass spectrum (MS) of oligo(*p*P-Se) ($n = 6$) (Fig. 5a) shows the presence of ions with masses: 156, 232, 312 and 392 respectively, whereas MS oligo(*p*P-Se) ($n = 23$), (Fig. 5b) shows ions with masses: 156, 232, 312, 392, and additionally with 468, 546, 624 and 702 mass units respectively. This can be attributed to different short chain phenylene-Se fragments, assignments of which are given in Fig. 5. The presence of ions with masses 468–702 indicates that short chains oligo(*p*P-Se)s can be obtained by vacuum evaporation of high molecular, unsoluble oligo(*p*P-Se)s.

All synthesized oligomers in this paper are, to some extent, partially crystalline. The electron diffraction patterns of oligo(*p*P), oligo(*p*P-S) and oligo(*p*P-Se) are given as examples in Fig. 6. The S and Se atoms of an individual chain are arranged in zigzag fashion with about 110° angle at the S or Se atoms. The 110, 200, 210 and 002 (Miller indexes) reflections at 0.142, 0.160, 0198, and 0.30 nm^{-1}, respectively, can be clearly seen for oligo(*p*P). It shows that there is no difference between short and long chains poly(*p*-phenylene)s [35, 36]. The electron diffraction patterns for oligo(*p*P-T)s (4 : 1, 1 : 1, 1 : 4) show that these compounds have low crystallinity and are almost amorphous, like the oligo(*p*P-T)s that are synthesized electrochemically. The only effect of the crystallinity of oligomers is on the rate of iodine doping, where doping of amorphous samples occurs more quickly than for crystalline.

3.2. Optical properties of oligomers

All studied oligomers give rise to strong π-π^* absorption bands. Absorption spectra of oligo(*p*P-T)s (4 : 1) (1 : 1) and (1 : 4) are shown in Fig. 7. Increasing the number of thienylene groups causes shifting of absorption maxima towards lower energies. The decreasing of π-π^* energy transition in oligo(*p*P-T)s is nearly a linear function of phenylene to thiophene ratios (Fig. 8). The small deviation from the linearity for oligo(*p*P-T) (1 : 1) shows some excess of thienylene groups: 1 : 1.1 and 1 : 1.05 for long polymeric and oligomeric fractions, respectively. Elemental analysis and IR calculation [36] indicate that this perturbation may be a result of special arrangements of the thienylene groups leading to HOMO-LUMO gaps smaller than those in simple superimposition of parent compounds [21, 23]. Electronic (UV-vis) absorption spectra of oligo(*p*P), oligo(T) and fluorescence emission spectrum of oligo(PT)—dotted line in $CHCl_3$ are shown in Fig. 9. They exhibit absorption maxima at 290 and 434 nm for oligo(*p*P) and oligo(T), respectively, and long tails up to 520 nm (2.35 eV). Long tail absorption indicates the presence of conjugated chromophores along the chains of the oligomers. The absorption characteristics of other oligomers are collected in Table II.

All oligomers show strong emission fluorescence in liquid solutions ($CHCl_3$,THF), in air, and at room temperature, when they are excited at the maxima of their absorptions. Emission fluorescence spectra of oligo(*p*P-T)s (4 : 1) (1 : 1) and (1 : 4) are shown in Fig. 10. They have emission maxima at 476, 493 and 520 nm, respectively. Increase of thienylene groups causes shifting of emission maxima towards longer wavelengths (for oligo(PT) emission max = 529 nm, see Fig. 9). The energy displacements between the absorption and emission maxima (ΔE_{max}) for oligo(*p*P-T)s (4 : 1) (1 : 1) and (1 : 4) are 0.85, 0.71 and 0.63 eV, respectively. They are higher than for oligo(*p*P) and oligo *p*(T), which are 0.54 and 0.48 eV, respectively. The high Stokes shift for oligo(*p*P-T)s reflects the

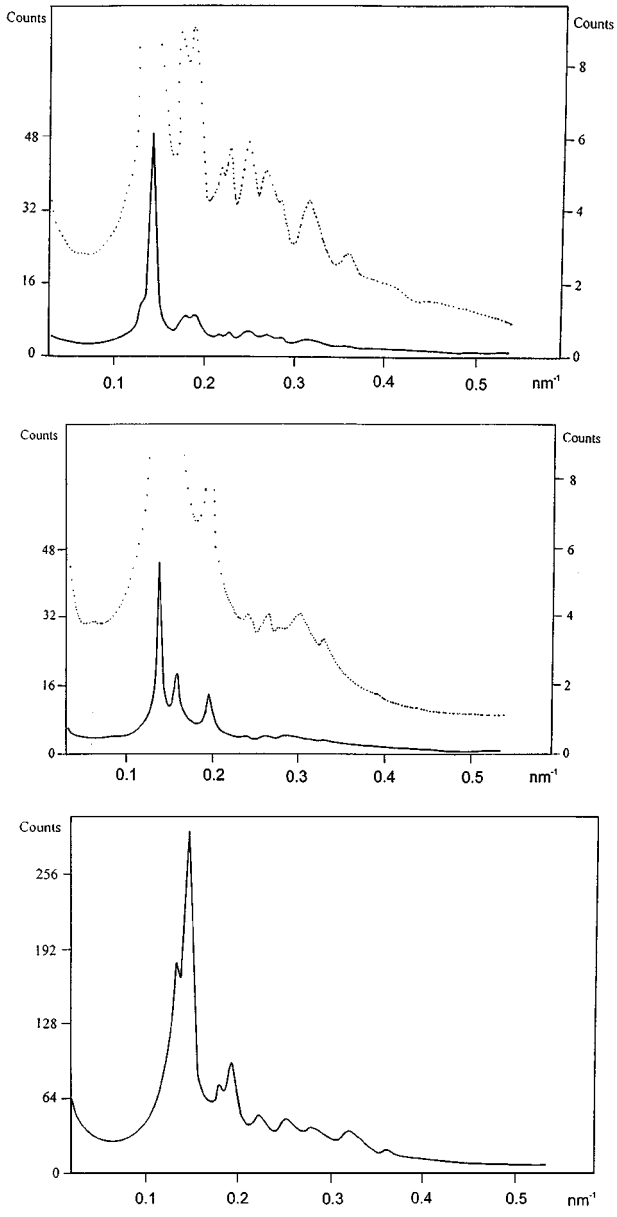

Figure 6 Electron diffraction patterns of: oligo(*p*P), oligo(*p*P-S) and oligo(*p*P-Se).

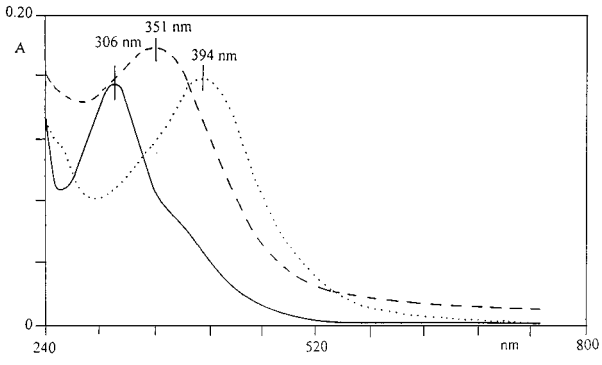

Figure 7 UV-vis absorption spectra of: oligo(*p*P-T): (-) 4 : 1; (- -) 1 : 1 and (. . .) 1 : 4.

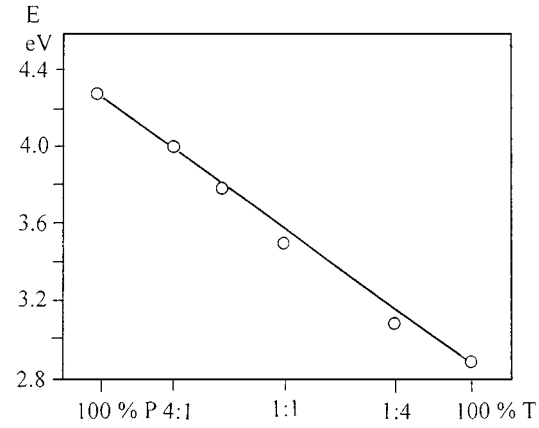

Figure 8 The π-π^* energy transition in oligo(*p*P-T) as a function of phenylene (P) and thiophene (T) components.

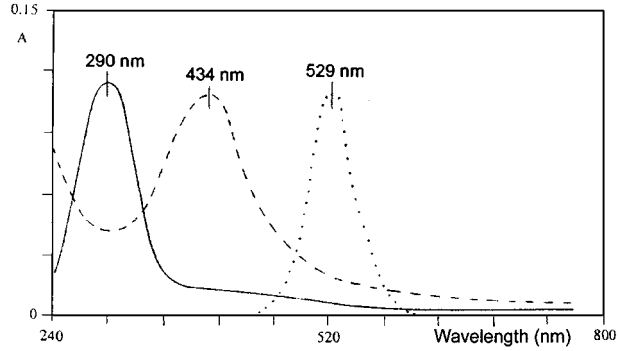

Figure 9 The UV-vis absorption spectra of oligo(*p*P) (-), oligo(pT) (—) and emission spectrum of oligo(*p*T) (. . .).

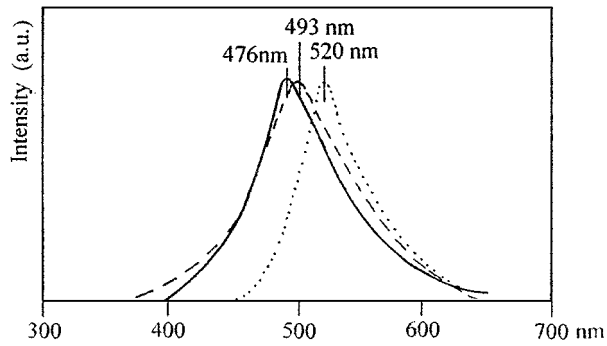

Figure 10 Emission fluorescence spectra of: oligo(*p*P-T)s (4 : 1) (1 : 1) and (1 : 4), respectively.

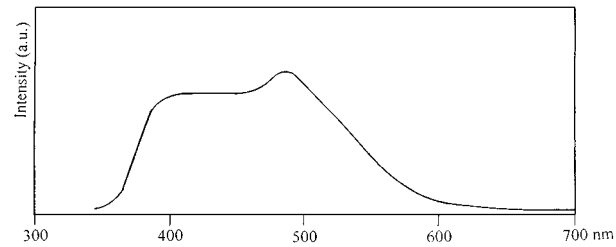

Figure 11 Emission spectrum for the mixture of oligo(*p*P-T).

strong contribution from the shorter chains (blue-shift of absorption maximum). The transfer towards the lowest π-π^* (longer chains) excitation energy and excitation migration, may give rise to the high Stokes shift observed [23, 37, 38]. The emission characteristics for other oligomers are collected in Table II.

The mixture of different oligo(*p*P-T) (4 : 1) (1 : 1) (1 : 4) in equimolar ratios in $CHCl_3$ solvent gives an additive, broad emission spectrum (Fig. 11). This observation has important impact for the potential application of these mixtures of oligomers in optoelectronics.

TABLE II UV-vis absorption and fluorescence emission characteristics for different oligomers

Sample	Absorption max (nm)	Fluorescence max (nm)	Excutation max (nm)	Absorption max (eV)	Edge absorption (eV)	Width of the fluorescence max (eV)	Difference between absorption max and fluorescence max (eV)
oligo(T)	434	529	469	2.90	2.35	0.32	0.48
oligo(*p*P)	290	398	363	4.30	3.15	0.34	0.54
oligo(*p*P:T) = 4 : 1	306	476	419	4.05	3.10	0.42	0.85
oligo(*p*P:T) = 1 : 1	351	493	438	3.55	2.65	0.43	0.71
oligo(*p*P:T) = 1 : 4	394	520	462	3.15	2.45	0.37	0.63
oligo(*p*P-S)	282	393	390	4.40	3.35	0.37	0.55
oligo(*p*P-Se)	276	384	371	4.50	3.45	0.36	0.54
oligo(*p*DP-S)	299	401	400	4.15	3.05	0.10	0.51
oligo(*p*DP-Se)	292	381	379	4.25	3.15	0.10	0.44

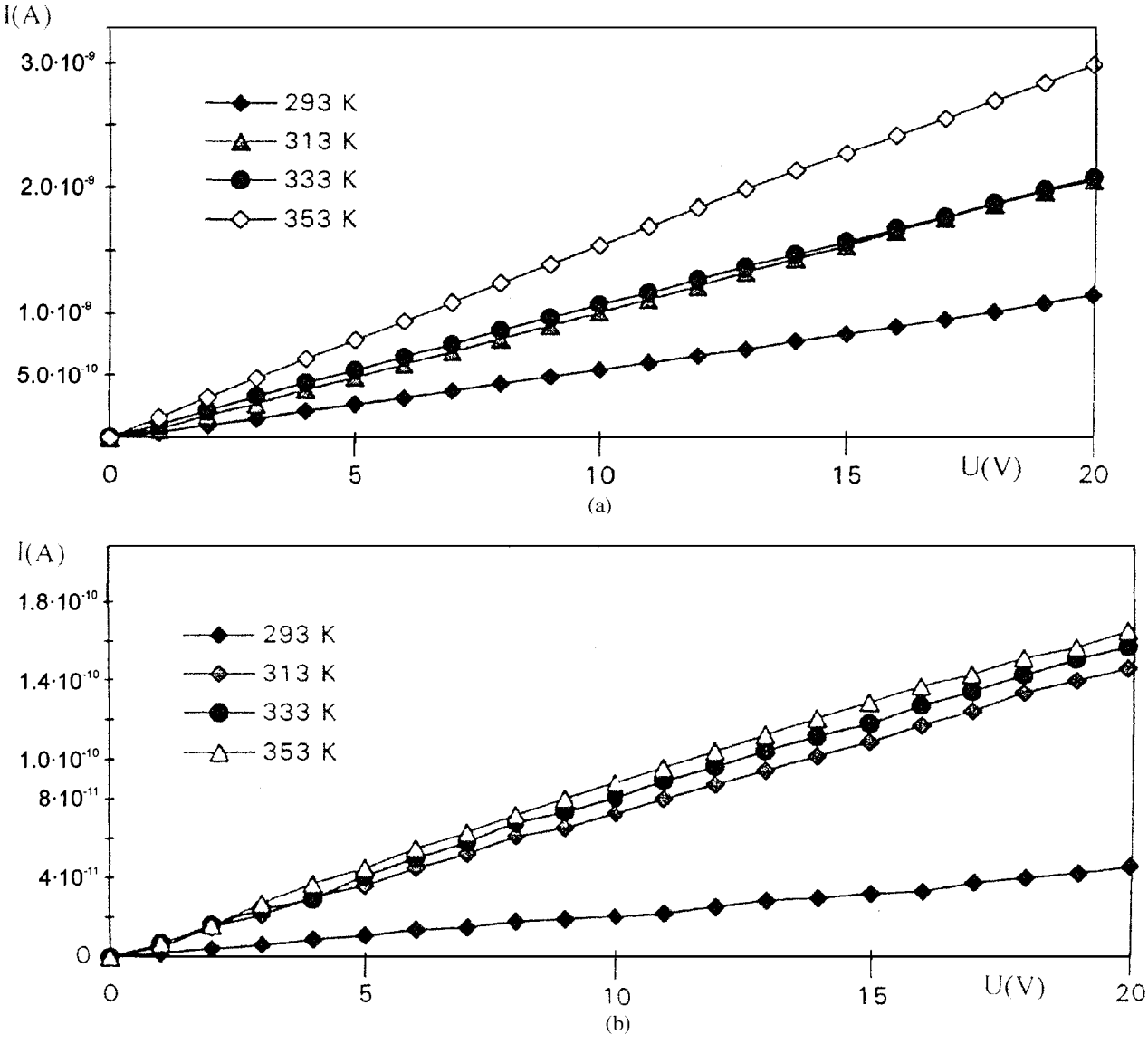

Figure 12 Current (*A*)-voltage (*V*) dependence for: (a) oligo(*p*P-T) (4 : 1) and (b) oligo(*p*P-S).

3.3. Electrical properties

The current-voltage characteristics, which characterize the quality of contacts in the Au-oligomer-Au sandwich, show a linear dependence of current vs. voltage in different temperatures for all studied oligomers. Examples of this dependence for oligo(*p*P-T) (4 : 1) and oligo(*p*P-S) are given in Fig. 12. Measurements at elevated temperatures show that all oligomers can be employed with electronic devices working at higher temperatures.

The conductivity of all oligomers is low. For oligo(*p*P-S), oligo(*p*P-Se), oligo(*p*D-S) and oligo(*p*D-Se), it varies between 10^{-9} and 10^{-11} S m^{-1}, and for oligo(*p*P) the conductivity (δ) is even lower. For oligo(T) and oligo(*p*P-T)s δ changes from 10^{-4} to 10^{-9} S m^{-1} (see Table III). The iodine doping of

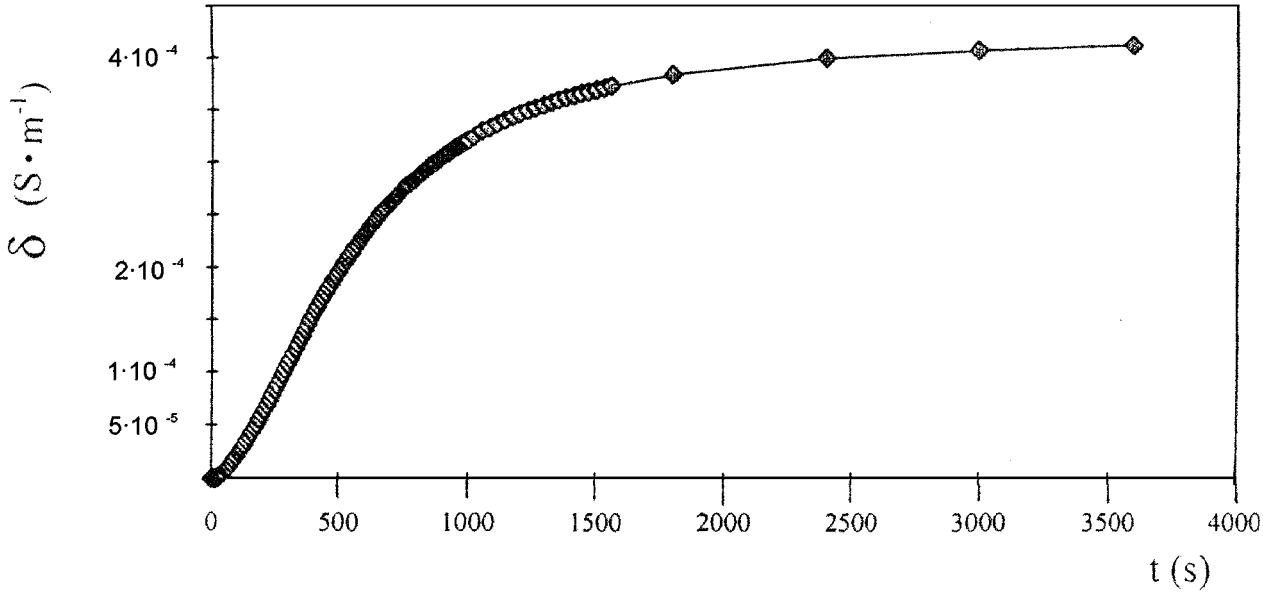

Figure 13 Electrical conductivity of: oligo(*p*P-T) vs. time of doping with iodine.

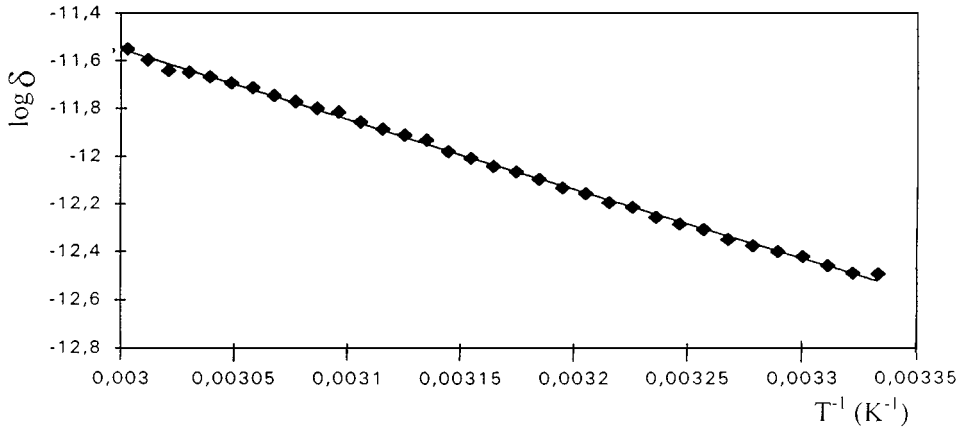

Figure 14 Temperature dependence of conductivity for: oligo(*p*P-T) (4 : 1).

TABLE III Electrical conductivities of undoped and iodine doped oligomers

	Conductivity (S m^{-1})	
Sample	Before doping	After doping
oligo(T)	3×10^{-4}	8700
oligo(*p*P)	$>10^{-12}$	10^{-12}
oligo(*p*P:T) = 4 : 1	10^{-9}	4×10^{-4}
oligo(*p*P:T) = 1 : 1	10^{-6}	30
oligo(*p*P:T) = 1 : 4	10^{-5}	1700
oligo(*p*P-S)	10^{-9}	10^{-6}
oligo(*p*P-Se)	10^{-10}	10^{-7}
oligo(*p*DP-S)	10^{-10}	10^{-7}
oligo(*p*DP-Se)	10^{-11}	10^{-8}

oligomers increase their conductivity, for example oligo(*p*P-T) (4 : 1) to more than 10^{-4} S cm^{-1} (Fig. 13) and oligo(*p*DP-S) to 10^{-7} S m^{-1}. The high conductivity observed in some polymeric semiconductors is due to delocalization of charge carriers along polymer chains. The process is enhanced when a polymer can adopt a planar configuration. Oligo(*p*P-S), oligo(*p*P-Se), oligo(*p*DP-S) and oligo(*p*DP-Se) are not planar because of bending of chains at sulfur and selenium atoms, and for that reason they have very low conductivity.

In the case of oligo(*p*P-T) (Fig. 13), the increase in conductivity is rapid during the first 10 min, followed by a slower increase, and after 25 min the conductivity level was constant. A different situation was observed for oligo(pDP-S) samples where the increase of conductivity was rather monotonic up to 120 min.

The temperature dependence of conductivity has also been investigated. An almost linear relation between $\log \delta$ and $1/T$ was observed for all oligomers. For oligo(*p*P), oligo *p*(T) and oligo(*p*P-T)s (4 : 1) (Fig. 14), (1 : 1) and (1 : 4), the linearity was very good with a correlation coefficient $r^2 = 0.99$. The correlation coefficient for oligo(*p*P-S), oligo(*p*P-Se), oligo(*p*DP-S) and oligo(*p*DP-Se) was a little lower ($r^2 = 0.97$). Such a behavior is consistent with tunneling of charge carriers between conducting regions [39] or with one-dimension hopping [40].

4. Conclusions

We have shown that π-conjugated low molecular oligomers because of their solubility can replace in-

soluble polymeric analogues. Thin conducting layers can be obtained by spraying or painting with solutions of oligomers which is a great advantage for optoelectronic industries. The bromine terminal groups in these oligomers give a possibility to attach them to longer block polymers with different energy gaps which is important from nonlinearity responses point of view.

Acknowledgements

The authors acknowledge the support of The Swedish Institute, who generously provided a post-doctorate stipendium to Dr. W. Czerwinski from the Faculty of Chemistry, Copernicus University in Torun, Poland.

References

1. T. A. SKOTHEIM (ed.), "Handbook of Conducting Polymers," (Marcel Dekker, New York, 1986).
2. J. L. BREDAS and R. SILBEY (eds.), "Conjugated Polymer: The Novel Science and Technology of Highy Conducting and Nonlinear Optically Active Materials" (Kluwer Academic Publishers, Dordrecht, Holland, 1991).
3. T. YAMAMOTO, *Prog. Polym. Sci.* **17** (1992) 1153.
4. H. G. KIESS (ed.), "Conjugated Conducting Polymers," Springer Series in Solid State Science (Springer-Verlag, Berlin, Heidelberg, 1992) p. 102.
5. J. H. BURROUGHES, C. A. JONES and R. H. FRIEND, *Nature* **335** (1988) 137.
6. A. TSUMARA, H. KOEZUKA and T. ANDO, *Synth. Met.* **25** (1988) 11.
7. G. HOROWITZ, X. PENG, D. FICHOU and F. GARNIER, *J. Appl. Phys.* **67** (1990) 528.
8. *Idem., J. Mol. Electronics* **7** (1991) 85.
9. G. HOROWITZ, *Adv. Mat.* **2** (1990) 287.
10. A. J. PAL, J. PALOHEIMO and H. STUBB, *Appl. Phys. Lett.* **67** (1995) 3909.
11. D. D. C. BRADLEY, A. R. BROWN, P. L. BURN, R. H. FRIEND, A. B. HOLMES and A. KRAFT, in "Springer Series in Solid State Sciences," Vol. 107, edited by H. Kuzmany, M. Mehring and S. Roth (Springer-Verlag, Berlin, 1992) p. 304.
12. G. GREM and G. LEISING, *Synth. Met.* **55–57** (1993) 4105.
13. A. J. PAL, T. OSTERGARD, J. PALOHEIMO and H. STUBB, *Appl. Phys. Lett.* **69** (1996) 1137.
14. T. OSTERGARD, J. PALOHEIMO, A. J. PAL and H. STUBB, *Synth. Met.* **88** (1997) 171.
15. A. J. PAL, T. OSTERGARD, J. PALOHEIMO and H. STUBB, *Phys. Rev. B* **55** (1997) 1306.
16. T. YOSHIMURA, *Opt. Commun.* **70** (1989) 535.
17. S. A. JENEKHE, W.-C. CHEN, S. LO and S. R. FLOM, *Appl. Phys. Lett.* **57** (1990) 126.
18. S. A. JENEKHE, *Chem. Mat.* **3** (1991) 878.
19. T. A. SKOTHEIM, R. L. ELSENBAUMER and J. R. REYNOLDS (eds.), "Handbook of Conducting Polymers," 2nd ed. (Marcel Dekker, Inc. New York, Basel, Hong Kong, 1998) pp. 165–196, and references therein.
20. F. MEYERS, A. J. HEEGER and J. L. BREDAS, *J. Chem. Phys.* **97** (1992) 2750.
21. D. A. DOS SANTOS, C. QUATTROCCHI, R. H. FRIEND and J. L. BREDAS, *ibid.* **100** (1994) 3301.
22. C. H. BOTTA, L. ROSSI, S. DESTRI and R. TUBINO, *Mol. Cryst. Liq. Cryst.* **256** (1994) 481.
23. W.-C. CHEN and S. A. JENEKHE, *Macromol.* **28** (1995) 465.
24. L.-A. LINDÉN, *Trends Polym. Sci.* **2** (1994) 144.
25. D. J. SANDMAN, M. RUBNER and L. SAMUELSON, *J. Chem. Soc. Chem. Commun.* **13** (1982) 1133.
26. W. CZERWINSKI, J. FINK and N. NUCKER, in "Electronic Properties of Conjugated Polymers," Springer Series of Solid State Sciences, edited by H. Kuzmany, M. Mehring, S. Roth (Berlin-Heidelberg, 1987) p. 330.
27. K. ERDMANN, W. CZERWINSKI, B. C. GERSTEIN and M. PRUSKI, *J. Polym. Sci. Part B: Polym. Phys.* **32** (1994) 1961.
28. J. FINK, *Z. Phys. B* **61** (1985).
29. S. KITAO, T. MATSUYAMA, M. SETO, YU. MAEDA, Y. F. HSIA, S. MASUBUCHI and S. KAZAMA, *Hyperfine Interactions*, **93** (1994) 1439.
30. S. LEFRANT, J. P. BUISSON and H. EKHARDT, *Synth. Met.* **17** (1991) 589.
31. A. SAKAMOTO, Y. FURAKAWA and M. TASUMI, *J. Phys. Chem.* **96** (1992) 3870.
32. M. AKIMOTO, Y. FURAKAWA, H. TAKEUCHI, I. HARADA, Y. SOMA and M. SOMA, *Synth. Met.* **15** (1986) 353.
33. G. LOUARN, J. P. BUISSON, S. LEFRANT and D. FICHOU, *J. Phys. Chem.* **99** (1995) 11399.
34. J. RONCALI, F. GARNIER, M. LEMARIE and R. GARREAU, *Synth. Met.* **15** (1986) 323.
35. W. CZERWINSKI, N. NUCKER and J. FINK, *ibid.* **25** (1988) 71.
36. W. CZERWINSKI, *ibid.* **35** (1990) 229.
37. J. O. OSAHENI and S. A. JENEKHE, *J. Am. Chem. Soc.* **117** (1995) 7391.
38. L. ROSSI, C. BOTTA, S. DESTRI, S. LUZZATI, A. BORGHESI and R. TUBINO, *Phys. Lett. A* **213** (1996) 288.
39. B. ABELES, *Appl. Solid State Sci.* **6** (1976) 1.
40. N. F. MOTT, "Metal-Insulator Transitions," (Taylor and Francis, London, 1974,) pp. 30–42.

Received 30 October 1997
and accepted 9 June 1999